PERFORMANCE OF AN ALL-NBN QUASI-OPTICAL SIS MIXER FOR THE TERAHERTZ BAND

Yoshinori UZAWA, Zhen WANG, Akira KAWAKAMI,
Kansai Advanced Research Center, Communications Research Laboratory,
588-2 Iwaoka, Iwaoka-cho, Nishi-Ku,
Kobe, 651-2492 JAPAN
e-mail: uzawa@crl.go.jp

and Shigehito MIKI
Graduate School of Science and Technology, Kobe University

Abstract

We designed an all-NbN SIS mixer with low-noise and wideband operation at terahertz frequencies. The mixer consists of a self-compensated NbN/AlN/NbN tunnel junction and an epitaxially grown NbN/MgO/NbN microstripline. The junction as a distributed element is 0.8 μm wide and 2.4 μm long, and its current density is 50 kA/cm^2. The microstripline consists of a 200-nm-thick NbN ground plane, a 180-nm-thick MgO insulator, and a 350-nm-thick NbN wiring layer. The frequency dependence of the receiver noise temperature was investigated by using an optically pumped far-infrared laser and backward-wave oscillators as local oscillators at frequencies from 760 to 980 GHz. The mixer showed flat noise characteristics at frequencies from 780 to 960 GHz, as predicted in our design process. The lowest receiver noise temperature was about 550 K at 909 GHz, including a 9-μm-thick Mylar beam splitter loss and other optical losses. Some large optical losses may be possible in the quasi-optical receiver configuration based on the standard method of input-loss estimation.

1. Introduction

Terahertz mixers with quantum limited noise sensitivity and wideband characteristics are needed in radio-astronomy projects, such as the Atacama Large Millimeter Array (ALMA), the Far-Infrared Space Telescope (FIRST), and so on. For the frequency bands above the gap frequency of Nb (about 700 GHz), for example, the ALMA specifies SSB noise temperatures of about 450 K for the band 10 (787-950 GHz, the relative bandwidth is 18.8%), and the FIRST needs low-noise SIS mixers for much higher frequency bands of up to 1.25 THz. Recently, SIS mixers consisting of conventional Nb/AlOx/Nb and Nb/AlN/NbTiN tunnel junctions and NbTiN-based tuning circuits have been developed and tested to enable low-noise operation at terahertz frequencies [1, 2]. However, these mixers had low-noise operation with DSB noise temperatures of 205 K at 798 GHz and 565 K at 970 GHz, their RF bandwidths were narrow due to the use of low-current density junctions (≅10 kA/cm^2). It was also found that heat trapping at the Nb/NbTiN interface degraded the junction properties, increasing the subgap leakage current and suppressing the gap voltage, which would degrade the noise performance [3].

We are currently developing SIS mixers based on NbN that have a high gap frequency of up to 1.4 THz. In principle, all-NbN SIS mixers should perform well below the gap frequency, just like all-Nb SIS mixers do. To develop wideband and low-noise mixers by designing all-NbN SIS mixers that can operate at terahertz frequencies, very high-current-density SIS junctions and

high-quality NbN films are needed to reduce the $\omega C_J R_N$ products and enable extremely low-loss transmission lines. For example, to cover the ALMA band 10 for below –10-dB matching, the maximum allowable value for $\omega C_J R_N$ products should be about 7 [4]. Assuming that the junction specific capacitance is 120 fF/μm^2, the required current density of the NbN tunnel junction should be about 40 kA/cm^2. Usually, the polycrystalline structure of NbN films is a problem because this structure has a large surface resistance on conventional insulators, such as SiO. This results in a large RF loss, which greatly degrades the mixer noise performance [5].

Another problem is that the relatively long penetration depth of NbN (even if NbN is a single crystal of, let's say 200 nm) makes the circuit design difficult because the large slow-wave factor shortens the circuits at terahertz frequencies. It was found that a conventional integrated tuning circuit did not work as effectively as it was designed to work because the spreading inductances introduced by the embedding of small junctions in the wide microstrip lengthened the tuning section [6]. As a result, there have been few reports of all-NbN SIS mixers with wideband and low-noise operation at teraherz frequencies.

Earlier, we developed NbN/AlN/NbN tunnel junctions epitaxially grown on MgO substrates that have current densities as high as 127 kA/cm^2 [7]. These tunnel junctions showed excellent noise performance at submillimeter-wave frequencies [8, 9]. Recently, we also developed NbN/MgO/NbN microstriplines epitaxially grown on a single-crystal MgO substrate that can be used in extremely low-loss tuning circuits [10]. In this report, we describe the design, fabrication, and testing of a quasi-optical SIS mixer with this NbN/MgO/NbN microstripline and a self-compensated NbN/AlN/NbN tunnel junction. This mixer dose not have a conventional tuning structure consisting of a microstrip inductor and a SIS junction as a lumped element [11].

2. Mixer Design

Our mixer uses an MgO hyperhemispherical lens, 3 mm in radius, with an antireflection (AR) cap. The AR cap is thermoformed Kapton JP polyimide film with a thickness of 50 μm, which corresponds to the thickness of a quarter-wavelength at around 800 GHz [5]. An optical micrograph of our mixer chip is shown in Fig. 1. A rectangular NbN/AlN/NbN junction and an NbN wiring on an MgO insulator were integrated with an NbN log-periodic antenna on a 0.3-mm-thick single-crystal MgO substrate. Because the NbN/MgO/NbN microstripline and the high-current-density NbN/AlN/NbN tunnel junction were grown epitaxially [12], we assumed in the mixer design process that the upper and lower NbN films had the same gap frequency of 1.27 THz and a normal state conductivity of 1.5 x 10^6 Ω^{-1}m^{-1}. These values were obtained from our measurements.

We designed the tuning circuit so that it had a center frequency of 1 THz. In this frequency region, NbN-based μm-sized SIS junctions must be considered as distributed elements, not lumped elements, because the slow-wave factor in these junctions is much larger than that in Nb junctions [11, 13]. This means that an NbN junction must be treated as a microstrip transmission line with a quasi-particle tunneling loss. It is well known that an imaginary part of the impedance in transmission lines becomes zero at a length of $n \times \lambda/4$, where n is an integer. For distributed SIS junctions, this means that the junction capacitance is tuned out, and the input impedance becomes the only real component. The impedance must be the largest at the $\lambda/2$ length for an open-ended junction. We calculated the size of the junction, including the NbN/MgO/NbN microstrip overhanging layer, as shown in Fig. 2. For the calculations, the distributed series impedance per unit length, *Z*, and the distributed shunt admittance per unit

length, Y, must be known. For a given distributed-SIS-junction geometry, Z and Y are defined as

$$Z = j\omega\mu_0 \frac{s}{W_J} + \frac{1}{W_J}(Z_{SU} + Z_{SL}) + j\omega\mu_0 \frac{d}{W_S - W_J} + \frac{1}{W_S - W_J}(Z_{SU} + Z_{SL}), \quad (1)$$

$$Y = \frac{W_J}{R_{rf}} + j\omega C_S W_J + j\omega\varepsilon_r\varepsilon_0 \frac{W_S - W_J}{d}, \quad (2)$$

where Z_{SU} and Z_{SL} are, respectively, the surface impedance of the upper and lower electrodes calculated from the Mattis-Bardeen theory of the anomalous skin effect [11], W_J and W_S are the widths of the NbN/AlN/NbN junction and the NbN/MgO/NbN microstripline, respectively, and R_{rf} represents the specific resistance of the quasi-particle loss due to the tunneling current through the insulator. The specific junction capacitance in pF/μm^2, C_S, was calculated based on the following equation obtained from the measurements of our high-current-density NbN/AlN/NbN tunnel junction:

$$\log C_S = 0.16 \log J_C - 1.15, \quad (3)$$

where J_C is the current density in kA/cm^2. The tunneling barrier thickness, s, was assumed to be 1 nm based on the observation of the high-current-density junction by using a transmission electron microscope (TEM) [12]. We used the relative dielectric constant, ε_r, of 9.6 for MgO, and the thickness was expressed as d.

The input impedance of this lossy transmission line was calculated using the parameters described in Table I. We decided that the width of the junction should be small to prevent transverse mode propagation. Figure 2 shows the real and imaginary parts of the input impedance. It can be seen that the junction capacitance is self-compensated at around 1 THz, i.e., the imaginary part becomes zero, while the real part becomes the maximum value of about 11 Ω. This relatively large resistance can be easily matched to the source impedance of the log-periodic antenna on the MgO lens (about 80 Ω) by using a λ/4 impedance transformer. The 13.5-μm length of the NbN/MgO/NbN microstripline enables good matching of below –10 dB at frequencies ranging from 900 to 1080 GHz, as shown in Fig. 3. Theoretically, a relative bandwidth of 18% can be achieved at terahertz frequencies.

3. Results and Discussion

A. Fabrication and I-V Measurements

The mixer chips were prepared by the fabrication process described in [14]. First, NbN/AlN/NbN trilayers were deposited in situ on an ambient-temperature MgO substrate by rf-magnetron sputtering in a load-locked sputtering system. One side of the antennas was formed by conventional photolithography and reactive ion etching (RIE). Then, rectangular junctions were defined using photolithography and RIE. After the MgO films were deposited by rf- and dc-magnetron sputtering to electrically insulate the base electrodes and the contact-wiring layer [10], an NbN film was deposited and patterned on the other side of the antennas and the contact-wiring layer to form a tuning circuit and to make contact with the junction. The actual thicknesses of the lower NbN, the lower MgO, and upper NbN were 200, 180, and 350 nm, respectively. The measured width was about 1.4 μm. The Josephson critical current of the junction was 950 μA at 4.2 K, and the junction was 0.8 μm wide and 2.4 μm long. This resulted in a current density of about 50 kA/cm^2. In the liquid helium measurement, we observed a slightly lower gap voltage of about 5 mV with backbending characteristics because of the large current through the junction. The normal state resistance was about 4 Ω.

To roughly define the tuning frequency, we also observed resonance-induced Josephson steps, as shown in Fig. 4. A dc current step could be seen at a voltage of about 1.9 mV, which corresponds to 920 GHz according to the Josephson frequency relationship, $f_J = 2eV_0/h$. This result indicates that the tuning frequency was slightly lower than the design frequency of 1 THz, because the fabricated junction was a little bit longer and the overhanging layer was a little bit narrower than the design junction and layer.

We analyzed the properties of the tuning circuit at terahertz frequencies by monitoring the dynamic resistance of the photon-assisted tunneling (PAT) steps induced on the *I-V* curves by a backward-wave oscillator (BWO). Figure 5 shows the pumped *I-V* curves at the RF irradiation of 900, 990, and 1030 GHz. As can be seen, there were changes in the dynamic resistance of the *I-V* curves at the PAT steps indicating that the capacitance of the junction was tuned out toward the lower frequency of 900 GHz.

B. Noise Measurements

The heterodyne receiver noise measurements were cunducted using the standard *Y*-factor method for room-temperature (295 K) and liquid-nitrogen-cooled (77 K) loads used as signals. The receiver set-up was basically the same as the one described in [5], except that an isolator was used instead of the 180-degree hybrid coupler. Local-oscillator (LO) power was introduced into the signal path through 9-μm and 16-μm-thick Mylar beam splitters. The signal and LO entered the dewar through a 0.5-mm-thick Teflon vacuum window, and the Zitex infrared filters cooled to 77 and 4.2 K. No corrections were made for the losses in front of the receiver.

Figure 6 shows the *I-V* characteristics of the receiver at 909 GHz with and without the LO power. The LO source was the BWO, and the 9-μm-thick Mylar beam splitter was used. As can be seen there was a suppression of the gap voltage in the pumped *I-V* curve. In addition, the width of the voltage measured at the PAT step, which was 3.25 mV, was narrower than the estimated width of 3.76 mV. These results show that the SIS junction suffered from the heating effects of the applied DC and RF power, because NbN has a low thermal conductivity. This local overheating increased the sub-gap leakage current of the junction and the loss in the NbN electrodes, which would degrade the noise performance. To reduce this heating effect, a normal metal, such as Al, should be deposited on the top electrode [15]. Figure 6 also shows the receiver IF output in response to the hot and cold loads as a function of the bias voltage. At voltages above the half-gap voltage of about 2.7 mV, the maximum *Y*-factor was about 1.25, which corresponded to the double-sideband (DSB) receiver noise temperature of 800 K. Below the half-gap voltage, the *Y*-factor was 1.35 (550 K) at 2.2 mV. However, the IF outputs around the first-Shapiro-step voltage of 1.88 mV were not stable because of the high dynamic resistance of the pumped *I-V* curve, as mentioned above. To obtain a better performance, a stronger magnetic field should be applied to the junction to suppress unwanted noise resulting from the Josephson effect.

The frequency dependence of the receiver noise temperature was investigated at frequencies ranging from 760 to 980 GHz. We used two BWOs for the 800-980 GHz measurements and an optically pumped CH_2F_2 far-infrared laser for the 760- and 783-GHz measurements. Figure 7 shows the receiver noise temperature as a function of the LO frequency. The 16-μm-thick Mylar beam splitter was used at all the measured frequencies, and a bias voltage was applied to the junction above the half gap to obtain stable operation. Wideband and flat-noise characteristics were observed at frequencies ranging from 780 to 960 GHz. Although the measured center

frequency of about 870 GHz was lower than the design frequency, the characteristics of the tuning bandwidth were almost consistent with the design ones, which means that the NbN films fabricated for the tuning circuits had no significant losses at terahertz frequencies. The fact that the center frequency was slightly lower than the observed resonance frequency of 920 GHz may be attributed to the increase in the effective penetration depth of the NbN due to the increase in the effective temperature in the NbN films by the DC and LO power.

At the higher and lower ends of the tuning frequencies, we could apply a bias voltage below the half-gap easier because the dynamic resistance of the pumped *I-V* curve became slightly smaller than that around the center frequency. Figure 8 shows the heterodyne response at 809 GHz when the 16-μm thick Mylar beam splitter was used. The maximum *Y*-factors below and above the half-gap voltage were, respectively, 1.33 (584 K) and 1.22 (914 K), including the Mylar-beam-splitter loss and other optical losses. Using the intersecting lines technique [16, 17], we estimated the input loss around this frequency from the IF responses biased below the half-gap voltage. A large input-noise contribution of about 350 K was derived that included the loss from the 16-μm-thick Mylar beam splitter. The most likely reasons for the high input noise are the following.

1) In the fabricated log-periodic antenna structure, at terahertz frequencies, the size of the teeth in the active region on the base (ground) side of the antenna was approximately 15% smaller than that on the other (wiring) side, due to shrinking by overetching. This unsymmetrical antenna structure results in an impedance mismatch and a poor beam pattern.
2) The loss of the thick MgO lens reduces the coupling efficiency at terahertz frequencies.

Using a high-efficiency input-coupling configuration, such as a waveguide structure, can improve the performance. We believe that all of the improvements described here can reduce the noise temperatures. We also believe that self-compensated NbN/AlN/NbN junctions and NbN/MgO/NbN microstriplines are more capable of low-noise and wideband operation at terahertz frequencies of up to 1.4 THz than conventional mixers that use lumped elements.

4. Conclusion

We designed, fabricated and tested at terahertz frequencies an all-NbN SIS mixer that has no conventional tuning structure. We demonstrated that tuning circuit, which consisted of a self-compensated NbN/AlN/NbN tunnel junction and an NbN/MgO/NbN microstripline, had effective low-noise and wideband operation in the terahertz band. The mixer had a simple structure and was fabricated by using conventional photolithography. Our fabricated NbN device remained stable throughout more than ten repetitions of the thermal cycle. We believe that the all-NbN SIS mixers with these excellent characteristics can be effectively used in projects, such as the ALMA, FIRST, and so on.

Acknowledegments

We thank Prof. V. Yu. Belitsky of Chalmers Univ. of Tech. for helpful suggestions about the tuning circuit and valuable discussions of the results. We thank Prof. T. Noguchi of the Nobeyama Radio Observatory and Dr. J. Inatani of NASDA for their constructive comments on the results. This work was supported in part by the ALMA Joint Research Fund of the National Astronomical Observatory of Japan.

References

[1] J. Kawamura, J. Chen, D. Miller, J. Kooi, J. Zmuidzinas, B. Bumble, H. G. LeDuc, and J. A. Stern, *Appl. Phys. Lett.*, vol. 75, pp. 4013-4015, 1999.

[2] B. D. Jackson, N. N. Iosad, G. Le Lange, A. M. Baryshev, W. M. Laauwen, J.-R. Gao, and T. M. Klapwijk, Submitted to *IEEE Trans. Appl. Supercond.*, March 2001.

[3] B. Leone, B. D. Jackson, J.-R. Gao, and T. M. Klapwijk, *Appl. Phys. Lett.*, vol. 76, pp. 780-782, 2000.

[4] A. R. Kerr, *IEEE Trans. Microwave Theory Tech.*, vol. 43, pp. 2-13, 1995.

[5] Y. Uzawa, Z. Wang, and A. Kawakami, *Appl. Supercond.*, vol. 6, pp. 465-475, 1998.

[6] B. D. Jackson, G. de Lange, W. Laauwen, J. R. Gao, N. N. Iosad, and T. M. Klapwijk, in *Proceeding of the 11th International-Symposium on Space Terahertz Technology*, University of Michigan, Ann Arbor, MI, 1-3 May 2000 (unpublished).

[7] Z. Wang, H. Terai, A. Kawakami, and Y. Uzawa, *IEEE Trans. Appl. Supercond.*, vol. 9, pp. 3259-3262, 1999.

[8] Y. Uzawa, Z. Wang, and A. Kawakami, *Appl. Phys. Lett.*, vol. 69, pp. 2435-2437, 1996.

[9] Y. Uzawa, Z. Wang, and A. Kawakami, *Appl. Phys. Lett.*, vol. 73, pp. 680-682, 1998.

[10] A. Kawakami, Z. Wang, and S. Miki, Submitted to *IEEE Trans. Appl. Supercond*., March 2001.

[11] V. Yu. Belitsky and E. L. Kollberg, *J. Appl. Phys.*, vol. 80, pp. 4741-4748, 1996.

[12] Z. Wang, H. Terai, A. Kawakami, and Y. Uzawa, *Appl. Phys. Lett.*, vol. 75, pp. 701-703, 1999.

[13] V. Yu. Belitsky and E. L. Kollberg, in *Proceeding of the 7th International-Symposium on Space Terahertz Technology*, University of Virginia, Charlottesville, VA, 12-14 March 1996 (unpublished).

[14] Z. Wang, A. Kawakami, Y. Uzawa, and B. Komiyama, *Appl. Phys. Lett.*, vol. 64, pp. 2034-2036, 1994.

[15] P. Dieleman, T. M. Klapwijk, S. Kovtonyk, and H. van de Stadt, *Appl. Phys. Lett.*, Vol. 69, pp. 418-420, 1996.

[16] R. Blundell, R. E. Miller, and K. H. Gundlach, *Int. J. IR & MM Waves*, vol. 13, pp. 3-16, 1992.

[17] Q. Ke and M. J. Feldman, *IEEE Trans. Microwave Theory Tech.*, vol. 42, pp. 752-755, 1994.

Table. 1 Parameters used in the design.

NbN upper electrode thickness:		200 nm
NbN lower electrode thickness:		200 nm
MgO insulator thickness, *d*:		200 nm
NbN/AlN/NbN junction width, W_J:		0.7 μm
	length:	2.25 μm
	current density, J_C:	40 kA/cm^2
	$J_C R_N A$ products	350 kVμm^2/cm^2
NbN/MgO/NbN microstripline width, W_S:		1.7 μm

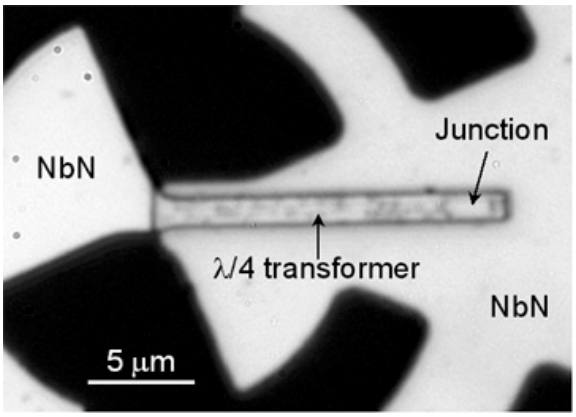

Fig. 1. Optical micrograph of the mixer. A rectangular NbN/AlN/NbN tunnel junction, as a distributed element, and a λ/4 NbN/MgO/NbN microstrip-impedance transformer were integrated with a self-complementary NbN log-periodic antenna.

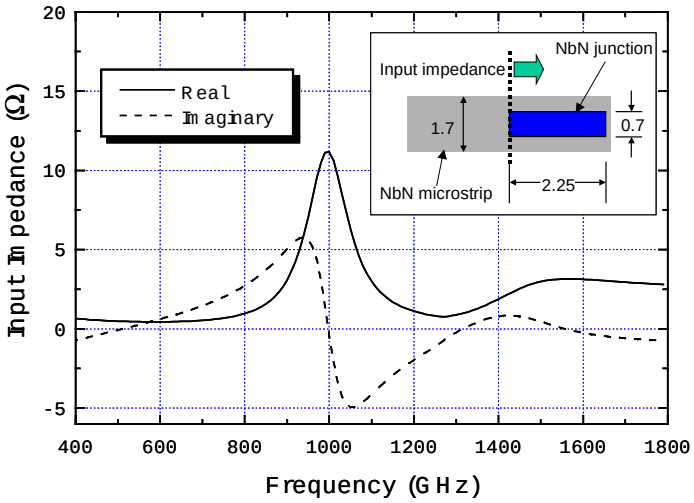

Fig. 2. Input impedance of the self-compensated junction tuning circuit. The junction capacitance was tuned out at the λ/2-wavelength frequency of 1 THz

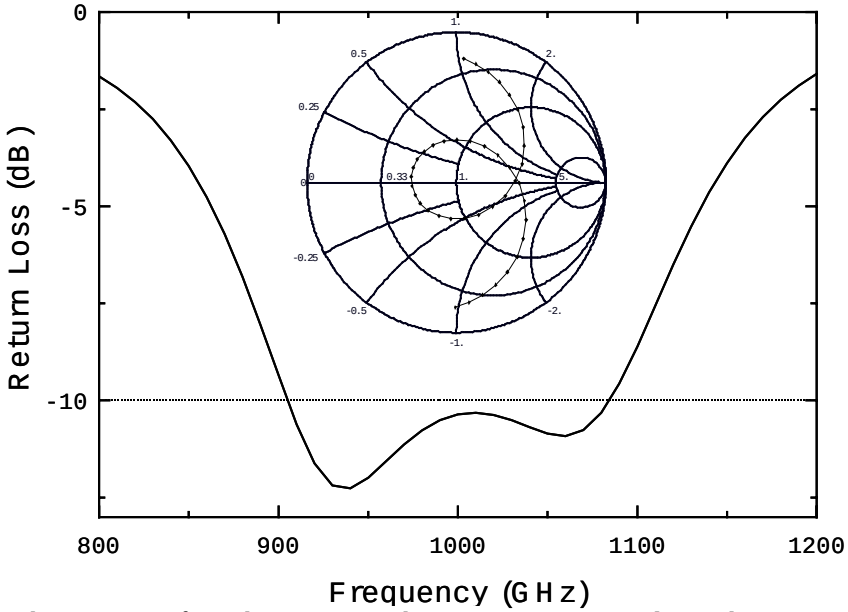

Fig. 3. Return-loss characteristics from the antenna to the tuning circuit. Impedance chart was normalized to the antenna source impedance of 80 Ω.

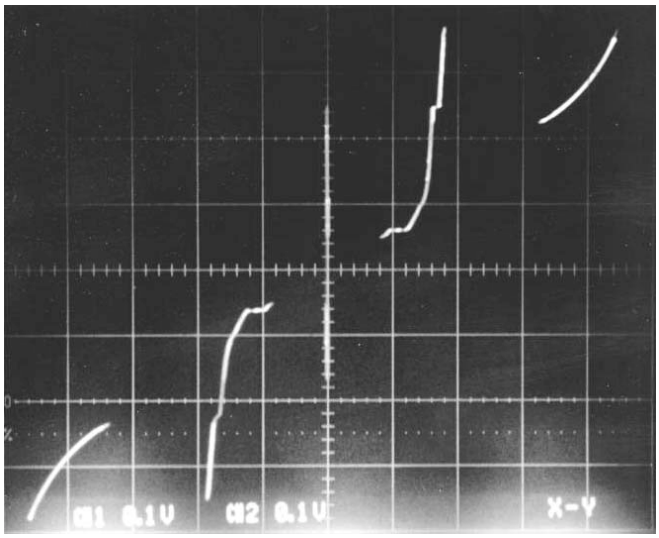

Fig. 4 Observed resonance-induced Josephson steps in the *I-V* curve. The horizontal scale is 1 mV per division, and the vertical scale is 0.1 mA per division.

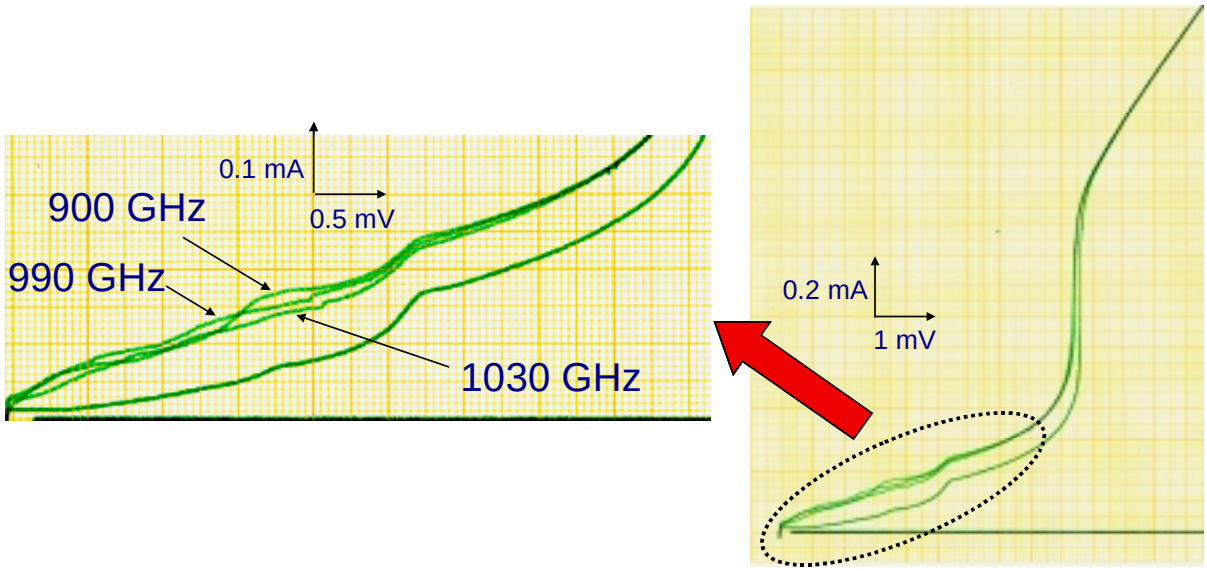

Fig. 5 Pumped I-V curves at the RF irradiation of 900, 990, 1030 GHz. Note that the changes in the dynamic resistance of the I-V curve at the PAT steps are visible.

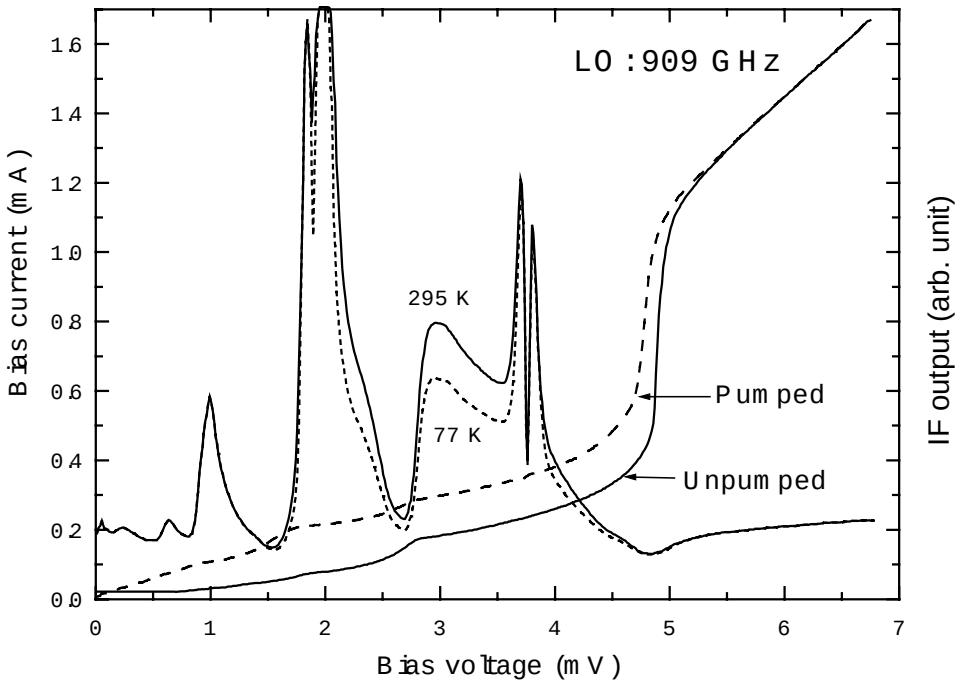

Fig. 6. Heterodyne response of the receiver at 909 GHz. Shown are the I-V characteristics for the self-compensated NbN/AlN/NbN tunnel junctions with and without the LO power. Also shown is the IF power as a function of the bias voltage for hot (295 K) and cold (77 K) loads.

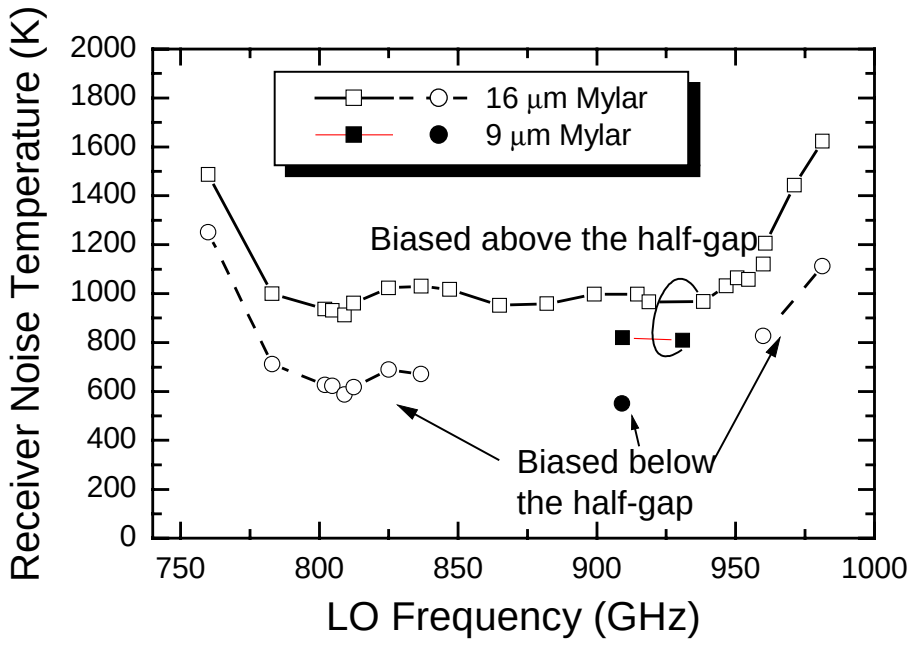

Fig. 7. DSB-receiver noise temperatures as a function of the LO frequency.

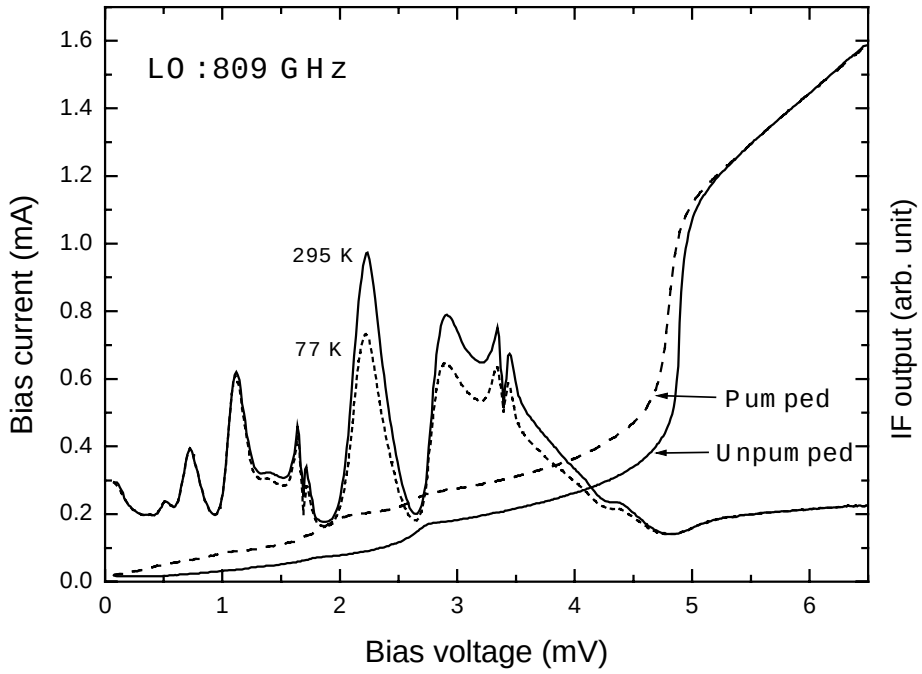

Fig. 8. Heterodyne response of the receiver at 809 GHz. Shown are the I-V characteristics for the self-compensated NbN/AlN/NbN tunnel junctions with and without the LO power. Also shown is the IF power as a function of the bias voltage for hot (295 K) and cold (77 K) loads.